Fibers and Polymers 2015, Vol.16, No.6, 1201-1212
DOI 10.1007/s12221-015-1201-8

ISSN 1229-9197 (print version)
ISSN 1875-0052 (electronic version)

Fabrication of PEO/Chitosan/PCL/Olive Oil Nanofibrous Scaffolds for Wound Dressing Applications

Amaneh Zarghami[1], Mohammad Irani[2], Amrolah Mostafazadeh[3], Monireh Golpour[3], Amir Heidarinasab[1], and Ismaeil Haririan[4,5]*

[1]*Department of Chemical Engineering, Sciences and Research Branch Islamic Azad University, Tehran 09821, Iran*
[2]*Department of Chemical Engineering, Amirkabir University of Technology, Tehran 15875-4413, Iran*
[3]*Departments of Cellular and Molecular Biology Research Center, Babol University of Medical Sciences, Babol 098-498, Iran*
[4]*Departments of Pharmacutics, School of Pharmecy, Tehran University of Medical Sciences, Tehran 14176-14411, Iran*
[5]*Medical Biomaterials Research Center (MBRC), Tehran University of Medical Science, Tehran 0098-21, Iran*
(Received January 4, 2015; Revised March 28, 2015; Accepted April 6, 2015)

Abstract: Biodegradable polyethylene oxide (PEO)/chitosan (CS)/poly(ε-caprolactone) (PCL)/olive oil composite nanofibers were fabricated by electrospinning process. The prepared nanofibers were characterized using SEM and FTIR analysis. A response surface methodology based on Box-Behnken design (BBD) was used to predict the average diameter of electrospun nanofibers based on electrospinning parameters including voltage, flow rate and tip-collector distance. The optimum experimental average diameter of electrospun nanofibers was found to be 86 nm which was in good agreement with the predicted value by the BBD analysis (88 nm). In vitro release of olive oil incorporated PEO/CS/PCL/olive oil nanofibers demonstrated a rapid release of olive oil during the first 3 h which enhanced gradually afterwards. Good attachment, spreading, cell proliferation, as well as nontoxic behavior of PEO/CS/PCL/olive oil nanofibrous scaffolds on HDF fibroblast cells were proved by cytotoxicity studies. Furthermore, the high antibacterial activity of PEO/CS/PCL/olive oil composite nanofibers against Gram-negative bacteria *E. coli* and Gram-positive *S. aureus* was observed. This study suggests that the prepared PEO/CS/PCL/olive oil composite nanofibrous scaffolds could be used as an ideal patch for wound dressing applications.

Keywords: Electrospinning, Olive oil, Composite nanofibers, Box-Behnken design, Antibacterial activity

Introduction

Electrospinning process is an effective method for fabrication of fibers in the range of micro or nano-sized diameters through an electrically charged jet of polymer or composite solution or polymer melt. Electrospun nanofibers due to the high porosity and large specific surface (area to volume ratio) with small pore size have a good potential for the biomedical applications [1,2]. In recent years, biocompatible nanofibers have been developed for different applications such as drug delivery systems [3-6], tissue engineering [7-10], wound dressing [11-14] and biomedical applications [15,16].

The various parameters such as concentration, viscosity, conductivity, surface tension of polymer solution, voltage, distance between needle tip and the collector (TCD), geometry of collector, temperature and humidity, control the electrospinning process. Investigation of each factor separately on the morphology of fibers would be very time consuming. Therefore, statistical experimental design methods can be used to evaluate the effects of variables and optimization of experimental parameters. Response surface methodology (RSM) is essentially a particular set of mathematical and statistical methods for experimental design and evaluating the effects of variables and searching optimum conditions of variables [17]. In recent researches, the factor space Central-Composite Design (CCD) and Box-Behnken Design (BBD) are commonly selected experimental design techniques [17]. However, for a quadratic response surface model with three or more factors, the BBD technique is much more advantageous compared with CCD [17].

In recent studies, natural polymers like chitin [18], chitosan [19], alginate, etc. due to their non-toxicity, enhanced biocompatibility and improvement the mechanical properties were often blended with synthetic polymers [20]. They were used in biomedical applications, like drug delivery, wound dressing and tissue engineering [20,21]. For example chitosan has excellent biological properties such as biodegradability, biocompatibility, nontoxicity, antimicrobial activity, wound-healing and scar-prevention properties. However, the electrospinning of chitosan due to the low solubility, low stability and low mechanical properties is extremely difficult. Therefore, the polymers such as polyethylene oxide (PEO), poly(vinyl alcohol), cellulose, zein, poly(lactic acid), ploy caprolactone (PCL) and Nylon-6 have been blended to chitosan to improve the mechanical properties of chitosan nanofibers [22]. Additionally, in order to decrease the water absorption capability, the electrospun chitosan nanofibers is cross-linked by triethylene glycol dimethacrylat [23], formaldehyde [24] and glutaraldehyde (GTA) vapor [25]. In this work, the PEO/chitosan nanofibers were fabricated by electrospinning process and were cross-linked by GTA.

*Corresponding author: haririan@tums.ac.ir

PCL due to unique properties such as nonimmunogenicity, slow biodegradability and good drug permeability have a high potential in tissue engineering, delivery system and biomedical applications [26,27]. Additionally, the natural biodegradable materials such as gelatin, beeswax, honey, herbs and olive oil could also be popular materials for the rapid recovery of cuts and burns [28]. Olive oil was used as a local choice for treatment of partial thickness burns [29]. Olive oil contains a high percentage of monounsaturated fatty acids and can potentially help restoring the permeability barrier. Olive oil also contains vitamin E and phenol compounds such as hydroxytyrosol, tyrosol, oleuropein, 1-acetoxypinoresinol, and (+)-pinoresinol, which are known to have powerful antioxidant potential [29]. However, olive oil due to the hydrophobic characteristic was insoluble in hydrophilic solution. Therefore, PCL as a biocompatible hydrophobic polymer is blended with olive oil.

In this study, the electrospinning technique was used to produce the PEO/chitosan/PCL/olive oil composite nanofibrous scaffolds. The effect of electrospinning parameters such as TCD, flow rate and applied voltage, on the morphology and diameter of electrospun nanofibers were determined. The morphology properties, degree of swelling and drug-release behavior of the PEO/chitosan/PCL/olive oil composite nanofibrous scaffolds were evaluated. In addition, HDF fibroblast cells were used to study cellular compatibility of the nanofibrous structure for potential use in wound dressing. Finally, the potential application of these composite nanofibers as antibacterial materials was examined using antibacterial test.

Experimental

Materials

Chitosan (75-85 % deacetylated, average Mw: 200,000), PEO (average Mw: 900,000) and PCL (average Mw: 80,000) were obtained from Sigma-Aldrich (Sigma-Germany). GTA, acetic acid, dichloromethane and methanol were purchased from Fluka (Fluka-Switzerland). Olive oil was provided from Elshan company (Elshan, Iran). Deionized water was used throughout this work.

Preparation of PEO/Chitosan and PCL/Olive Oil Solutions

The chitosan (3.5 % w/v) and PEO (3.5 % w/v) solutions were initially prepared separately by dissolving chitosan or PEO in 0.5 M acetic acid. Then, the PEO/Chitosan solution was obtained by blending of Chitosan and PEO with ratio of 9:1 and stirring at temperature of 25 °C for 24 h.

PCL/olive oil mixture was prepared by mixing PCL and olive oil in the mass ratio of 1:5 in a dichloromethane (DCM): methanol (7:3 v/v) solvent mixture under steering for 6 h at room temperature. In order to investigate the effect of olive oil concentration on the fibers diameter, olive oil with different concentrations with volume ratio of 1:10, 2:10 and 3:10 was added to the PCL solution.

Electrospinning Process

The prepared PEO/chitosan and PCL/olive oil solutions were loaded into two 5 m*l* plastic syringes that were driven by individual two KD programmable syringe pumps to control the solution flow rate. Then the high voltage is applied between a needle and a collector to produce the PEO/chitosan/PCL/olive oil composite nanofibers on a collector.

Design of Electrospinning Experiments by Box-Behnken Design (BBD)

Three factors three levels Box-Behnken design (BBD) were used to determine the relation between variables containing applied voltage (15-25 kV), flow rate (0.2-1 m*l*/h) and TCD (7.5-20 cm) on the average diameter of PEO/chitosan/PCL/olive oil composite nanofibers. The experimental design and results are shown in Table 1.

The BBD response surface model of electrospinning experiments expresses the PEO/chitosan/PCL/olive oil composite nanofibers diameter as a function of the above mentioned variables. The polynomial model for the nanofibers diameter with respect to the electrospinning variables is expressed as follows in equation (1):

$$Y = \beta_0 + \sum_{i=1}^{3}\beta_i x_i^2 + \sum_{i=1}^{3}\beta_{ii} x_i^2 + \sum_{i=1}^{3}\sum_{j=1}^{3}\beta_{ij} x_i x_j \quad (1)$$

where Y is the predict response by the model and β_0, β_i, β_{ii}, β_{ij} are the constant regression coefficient of the model. X_i, X_{ii} and X_{ij} represent the linear, quadratic and interactive terms of

Table 1. The experimental design and results of PEO/CS/PCL/olive oil nanofibers diameter

Experiment number	Voltage X_1 (kV)	TCD X_2 (cm)	Flow rate X_3 (m*l*/h)	Fiber diameter (nm)	Predicted value by the model (nm)
1	15	7.5	0.6	131	130
2	25	7.5	0.6	112	114
3	15	20	0.6	120	117
4	25	20	0.6	115	114
5	15	13.75	0.2	102	104
6	25	13.75	0.2	93	94
7	15	13.75	1.0	114	115
8	25	13.75	1.0	107	105
9	20	7.5	0.2	108	106
10	20	20	0.2	98	99
11	20	7.5	1.0	118	118
12	20	20	1.0	108	111
13	20	13.75	0.6	95	94
14	20	13.75	0.6	96	94
15	20	13.75	0.6	95	94

the uncoded independent variables, respectively. The coefficient of determination (R^2) was used to evaluate the accuracy of the full quadratic equation.

Nanofibers Characterization

FTIR spectroscopy was used in the range 400-4000 cm^{-1} to determine the type of functional groups on the prepared nanofibers. Dried nanofibers were mixed with KBr powder and pelletized. The IR characterizations were performed using a Perkin-Elmer Spectrum GX FTIR spectrometer. The surface morphology of the electrospun nanofibrous scaffolds was examined with SEM (MV2300) after gold coating. The average diameter and diameter distribution of nanofibers were obtained with an image analyzer (Image-Proplus, Media Cybrernetics).

Cross-linking of Nanofibrous Scaffolds

There are some reports about improving hydrophilic property of chitosan based nanofibrous scaffolds by treating with 25 % GTA vapor [30]. In the present work, 25 % GTA vapor was used for cross-linking of PEO/chitosan/PCL/olive oil and PEO/chitosan nanofibrous scaffolds. The nanofibrous scaffolds were first treated with 25 % GTA vapor in desiccators for 24 h to eliminate their hydrophilic property. The fibers were dried for 12 h at 60 °C in a vacuum chamber. The cross linked nanofibrous scaffolds were then dipped in water for 24 h to verify their improvement in water insolubility.

Degree of Swelling and Weight Loss of Nanofibrous Scaffolds

All nanofibrous scaffolds were submerged in the release medium (acetate buffer aqueous solution, pH 5.5) at 37 °C for 24 h. The degree of swelling (DS) and weight loss (WL) of electrospun nanofibrous scaffolds were determined according to the following equations (2) and (3), respectively.

$$DC = \frac{W_{st} - W_{dt}}{W_{dt}} \tag{2}$$

$$WL\ (\%) = \frac{W_{di} - W_{dt}}{W_{dt}} \times 100 \tag{3}$$

where W_{st} is the weight of each swollen specimen after submersion in the acetate buffer medium which is wiped dry with filter paper. W_{dt} is the weight of the specimen in its dry state after submersion in the medium acetate buffer, and W_{di} is the initial weight of the specimen in its dry state.

In vitro Release

For study of release characteristics of the olive oil from the composite nanofibrous scaffolds, 150 mg of composite nanofibers were filled into a dialysis bag with a cut off 12000-14000 g mol^{-1}. Dialysis bag was filled with 5 m*l* of acetate buffer solution (pH 5.5). The bag containing nanofibers was then immersed into the 20 m*l* of the same acetate buffer solution at 37 °C. The solution was continuously stirred with a constant speed of about 200 rpm using magnet stirrer. At a specified time intervals (from 0.5 to 24 hrs), 3 m*l* of the buffer solution removed and was kept as a stock for absorption measurements. After removal of each sample, 3 m*l* of the same buffer at 37 °C was added to the initial volume to provide sink condition.

The olive oil release rate was determined using a UV spectrophotometer (Spekol 2000, Analytikjena). The maximum wavelength for olive oil in DMF solution was 270 nm.

Cell Culture Studies

To examine the attachment, proliferation and cytotoxicity effects of different combination of the scaffold and substrate (PCL, PCL/olive oil, cross-linked PEO/chitosan and cross-linked PEO/chitosan/PCL/olive oil) on human cell, three different fibroblast cells were isolated primary from human dermal fibroblasts (HDF). The cells were treated by culturing in DMEM high glucose (PAAE15-883) supplemented with 10 % fetal bovine serum (FBS, PAAA15-15), 1 % antibiotics penicillin and streptomycine (PAAP11-010) under standard conditions of 5 % CO_2 at 37 °C. The culture medium was changed every 3 days until passage 3 [31].

Cell Proliferation and Cytotoxicity Assay

The four types of above mentioned nanofibrous scaffolds were cut in to 14 mm^2 size and sterilized under UV light for 40 min and then washed with sterilized phosphate buffered saline solution (PBS, PAAH15-002) three times and then were transferred to 24-well cell culture plate (Orange 5530300). The fibroblasts at passage 3 were detached using Trypsin/EDTA solution (Gibco invitrogen) and were suspended in DMEM high glucose supplemented with 10 % FBS, %1 antibiotics penicillin and streptomycin. They were seeded with density of 5×10^3 cells per each well. The plates were then maintained for 24, 48 and 96 h inside in the incubator having %5 CO_2 at 37 °C. The culture medium was replaced every 2 days for providing them for MTT assay [32].

Cell Attachment Morphology

To investigation the attachment quality of fibroblast with the hematoxylin and eosin (H&E) staining, four types of nanofibrous scaffolds including PCL, PCL/olive oil, cross-linked PEO/chitosan and cross-linked PEO/chitosan/PCL/olive oil were used. After incubation the attached cell on the scaffolds for 24, 48 and 96 h, the scaffolds were treated with 2.5 % GTA for 20 min and then were washed by distilled water for 4 min. The samples were put in a special paint colored glass that was the core hematoxylin for 10 min, and scaffolds washing with Alkali water. Then the cells adhered to scaffolds were dehydrated in ethanol 95 %, and the cytoplasm were stained by eosin for 2 min each then were dehydrated in ethanol 70 % and allowed to dry. Then samples were dried naturally and cell morphology was also observed by an Olympus phase contrast microscope at

magnification (×400) (Model 1×70, Japan) [30].

Antibacterial Activity

The antibacterial activities of samples against *E. coli* , as a Gram-negative bacterium and *S. aureus* as Gram-positive bacteria were investigated by a zone inhibition method [33,34]. The 50 mg of nanofibrous scaffolds were formed into the center of plates. The nutrient agar plates were then inoculated with 1 m*l* of bacterial suspension containing around 10^5 colony forming units for each bacterium. The same amounts of samples were gently placed on the inoculated plates, and were subsequently incubated at 37 °C for 24 h. Lack of inhibitory zones implied that there were no antibacterial activities. Formation of inhibitory zones entailed antibacterial activities. The experiment was repeated three times.

Results and Discussion

Electrospinning Process

Effect of Electrospinnig Variables on Nanofibers Diameter

The effects of three experimental factors including voltage, flow rate and TCD on the diameter of the electrospun PEO/chitosan/PCL/olive oil composite nanofibers were evaluated at three levels (Table 1). The effect of flow rate on the diameter of electrospun fibers is shown in Figure 1(a). At flow rate lower than 0.2 m*l*/h, the spinning solution was dried and the electrospinning process was stopped. As shown in Figure 1(a), the diameter of fibers was increased and the distribution of fibers diameter was spread followed by increase in flow rate. It could be attributed to the decreasing of electrostatic density which in turn caused to fabricate the bead fibers with greater diameters in higher flow rates. Similar trends were presented by other researchers [35,36]. The effect of applied voltage on the formation of electrospun fibers in the range of 15 to 25 kV was shown in Figure 1b. At lower voltage, the electrical force was not enough to form the homogenous fibers. When the voltage was increased to 20 kV, the uniform thinner fibers were obtained. At higher voltage (25 kV), the high strength of the electrical field increased the instabilities of jet solution which led the fibers with larger diameters. Figure 1(c) shows the effect of TCD on the diameter of electrospun nanofibers. At lower TCD of 7.5 cm, beaded fibers were formed. This could be attributed to insufficient evaporation of the solvent before it reached the collector due to the decrease in the TCD. By increasing the TCD to 13.75 cm, the homogeneous fibers with lower diameters were produced due to adequate drying of the fibers before collection. However, at TCD of 20 cm, the strength of electrical force on the spinning solution decreased and fibers with higher diameters were formed.

Analysis of Experimental Design

Analysis of variance (ANOVA) was performed to evaluate a full quadratic response surface model. P-value is a measure

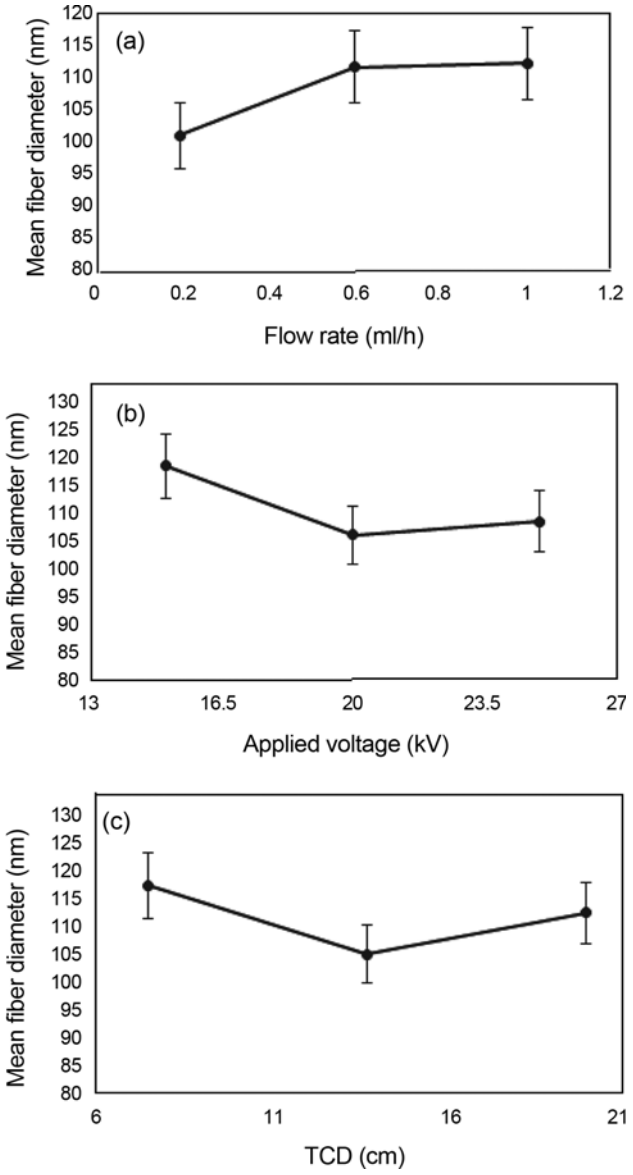

Figure 1. The Effect of (a) flow rate, (b) voltage, and (c) TCD on the diameter of electrospun PEO/chitosan/PCL/olive oil composite nanofibers.

of statistical significance and the electrospinning parameter shows significant impact on the average fiber diameter while the P-value is less than 0.05 at 95 % confidence interval. Table 2, revealed that linear terms , two quadratic terms and one of the interaction term (X_1X_2) exhibited significant effects on the average fiber diameter at $p<0.05$.

By elimination of insignificant terms ($p>0.05$) from the full quadratic model, the equation (2) which includes a series of linear, quadratic and interaction terms for the three electrospinning variables was designed, as follows:

$$Y\,(\text{nm}) = 94.462 - 5.000x_1 - 3.500x_2 + 5.570x_3 + 10.192x_1^2 + 14.192x_2^2 + 3.500x_1x_2 \quad (4)$$

Table 2. ANOVA results for the experimental response at different levels

Source	DF	Seq SS	Adj MS	F	P
Regression	9	1682.57	186.952	29.99	0.001
Linear	3	562.50	187.500	30.08	0.001
X_1	1	200.00	200.000	32.09	0.002
X_2	1	98.00	98.000	15.72	0.011
X_3	1	264.50	264.500	42.43	0.001
Square	3	1070.07	356.689	57.22	0.000
X_1^2	1	314.52	375.410	60.23	0.001
X_2^2	1	748.14	732.333	117.49	0.000
X_3^2	1	7.41	7.410	1.19	0.325
Interaction	3	50.00	16.667	2.67	0.158
$X_1 X_2$	1	49.00	49.000	7.86	0.038
$X_1 X_3$	1	1.00	1.000	0.16	0.705
$X_2 X_3$	1	0.00	0.000	0.00	1.000
Residual error	5	31.17	6.233		
Lack-of-fit	3	30.50	10.167	30.50	0.032
Pure error	2	0.67	0.333		
Total	14	1713.73			

The goodness-of-fit measure of the model was evaluated using the coefficient of determination (R^2). The high value of (R^2=0.976) indicated a high reliability of the model in predicting the average diameter of PEO/chitosan/PCL/olive oil composite nanofibers.

Response Surface Analysis

Figure 2(a)-(c) shows the 3D surface plots of the process parameters. Each figure indicates the simultaneous relation between the two parameters at the center level of third parameter. The surface plot for applied voltage versus flow rate (Figure 2(a)) showed that the lower flow rate and varying the applied voltage produced the smaller fiber diameter. Meanwhile, a small increase in diameters of fibers by increasing the voltage in the range of 20-25 kV at different flow rate was observed. Figure 2(b) showed the relation between the flow rate and TCD at the time on the fiber diameter. As shown, the lower TCD and higher flow rate had opposite effects on the electrospinning process resulted in ascending in the mean diameter of electrospun nanofibers. Also, it was observed that varying in TCD played fundamental role in the fiber diameter at different solution flow rates. The surface plot of predicted mean fiber diameter values versus applied voltage and TCD is shown in Figure 2(c). As shown varying of voltage and distance at the time was very important in the formation of electrospun nanofibers. This conclusion was also supported by the ANOVA table, which indicated that the interaction term between the applied voltage and distance was significant.

Optimization of PEO/Chitosan/PCL/Olive Oil Composite Nanofiber Diameter

In the electrospinng process, it is very important to obtain nanofibers with minimum diameter, because the thinner and homogeneous fibers provide maximum surface area and porosity, which is advantage for the higher loading of olive oil onto the composite nanofibers. By solving the equation (4), the optimal uncoded values of applied voltage, TCD and flow rate were estimated to be 21.20 kV, 14.30 cm and 0.20 ml/h, respectively. Thus, the minimum fiber diameter of composite nanofibers was found to be 88 nm. For identical electrospinning parameters, the experimental average nanofiber diameter value for three replicate was obtained as 86 nm, which was very close to the predicted value of nanofiber diameter calculated by the response model.

Validation of the Experimental and Predicted Model Data

The experimental average diameter of nanofibers was compared with the predicted values of the response model using the linear correlation coefficient (Figure 3(a)). As shown, the experimental values of composite nanofiber diameter were in close agreement with the predicted values of model. The value of adjusted correlation coefficient (Adj-R^2=0.92) indicated a reasonable relationship between the experimental data and model values. The probability distribution plot of residuals (difference between the model predicted fiber diameter values and those derived experimentally) is presented in Figure 3(b). As shown, the errors were normally distributed. Furthermore, it was observed that the established model was sufficient to estimate the average diameter of PEO/chitosan/PCL/olive oil composite nanofibers, as all the residuals were smaller than 5 %.

Degree of Swelling and Weight Loss of Nanofiber Mats

The effects of degree of swelling and the weight loss of

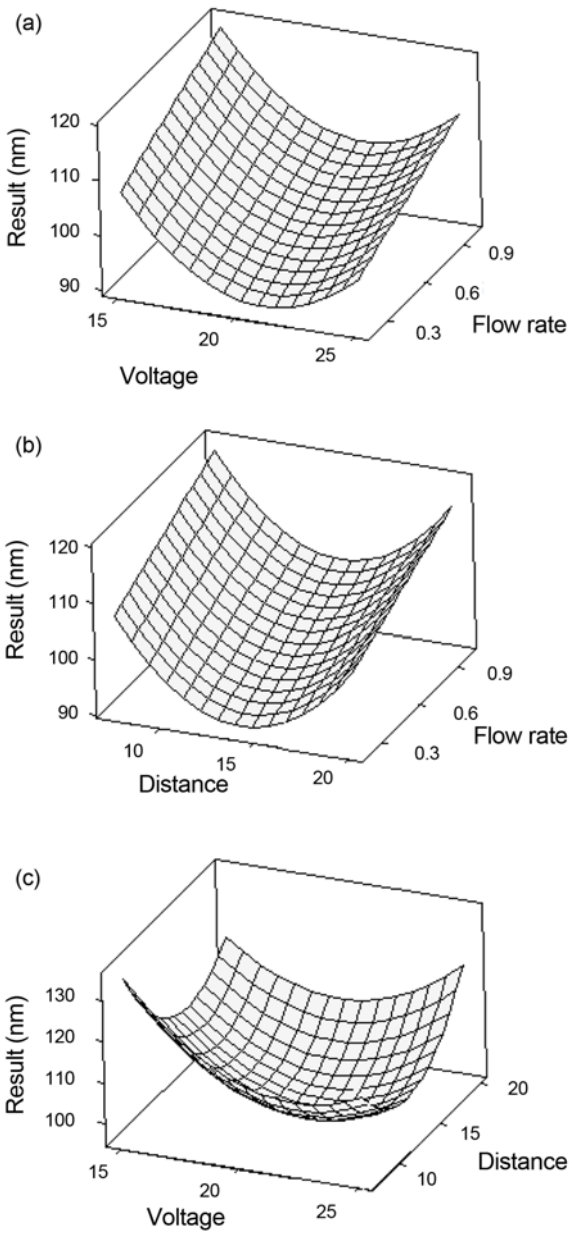

Figure 2. Surface plots of the response variable (fiber diameter (nm)) for the different experimental factors (twofactor- at-a-time (a) voltage and flow rate (b) flow rate and distance, and (c) distance and applied voltage on the diameter of PEO/chitosan/ PCL/olive oil nanofibrous scaffolds.

PEO/chitosan (non cross-linked), PEO/chitosan (cross-linked), PCL, PCL/olive oil, PEO/chitosan/ PCL/olive oil (non cross-linked), and PEO/chitosan/PCL/olive oil (cross-linked) nanofibrous scaffolds in the release medium (acetate buffer, pH 5.5 at 37 °C for 24 hrs) are illustrated in Figure 4. As shown in Figure 4(a), degrees of swelling of the nanofibrous scaffolds were in correct order owing to their hydrophilic-hydrophobic properties. The results indicated that the rate of

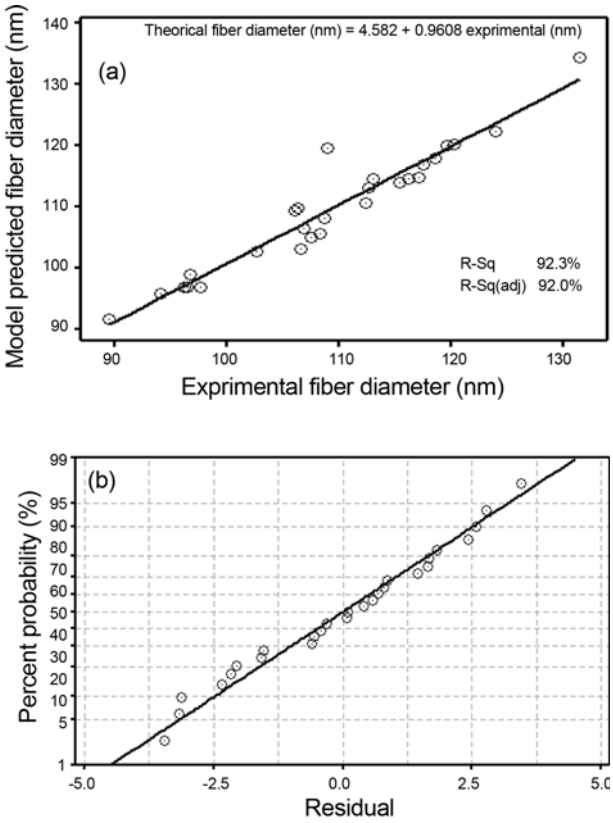

Figure 3. (a) Plot of model predicted fiber diameter against experimental fiber diameter and (b) normal probability plot.

water adsorption show a direct relation with the hydrophilic properties of the samples. The non cross-linked PEO/chitosan nanofibrous scaffolds had maximum swelling water absorption capability which decreased after cross-linking with moist GTA vapor for 24 hrs. High water absorption capability of the PEO/chitosan electrospun nanofibrous scaffolds could be due to the hydrophilic property of chitosan. The decrease in water absorption capability of the PEO/chitosan composite upon cross-linking with GTA could be attributed to the formation of aldimine linkages (-CH=N-) between the free amino groups of chitosan and the aldehyde groups of GTA [30]. These linkages caused adjacent fiber segments to fuse to one another and increased water diffusivity resistance and decreased water absorption capability. While the PCL nanofibrous scaffolds had minimum swelling because of its hydrophobic property, adding a plasticizer agent (e.g. Olive oil) to it, led to increase its water absorption capability. This was responsible for higher degree of swelling of PCL/olive oil nanofibrous scaffolds in comparison to PCL nanofibers. Generally, the more degree of swelling of nanofibrous scaffolds resulted in the penetration of more drugs in the release medium. On the other hand, the release rate increases with increasing degree of swelling of nanofibrous scaffolds. In addition, the wettability of the electrospun nanofibrous

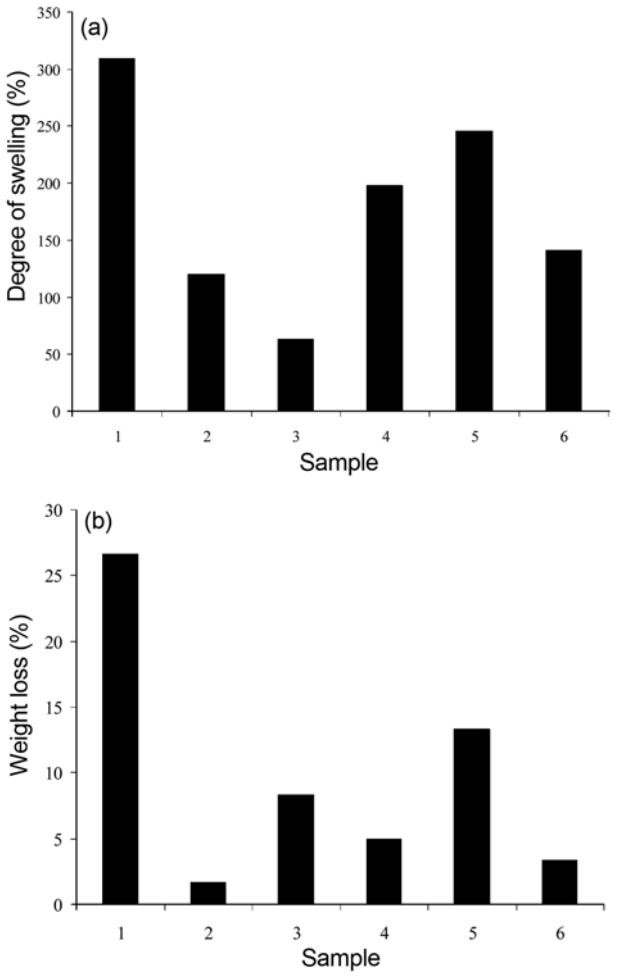

Figure 4. Effect of the type of polymer and/or olive oil a) on the degree of swelling (%) and (b) on the weight loss (%) of PEO/chitosan (noncross-linked)[1], PEO/chitosan (cross-linked)[2], PCL[3], PCL/olive oil[4], PEO/chitosan/PCL/olive oil (noncross-linked)[5], and PEO/chitosan/PCL/olive oil (cross-linked)[6] nanofibrous scaffolds.

scaffolds increases by enhancing of degree of swelling. As a result, the higher degree of swelling improves rate of wound healing. It should be noted that cells adhere and spread more effectively on surfaces with suitable hydrophilicity than on hydrophobic surfaces. Based on Figure 4(b), as expected, the non cross-linked PEO/chitosan and PEO/chitosan/PCL/olive oil nanofibrous scaffolds showed a greater weight loss than that of the cross-linked. The non cross-linked PEO/chitosan nanofibers indicated maximum weight loss/degradation (due to the hydrophilic property of chitosan) and its degradation was decreased after cross-linkage by moist GTA vapor during 24 hrs. The decrease in the percentage of weight loss of the nanofibrous scaffolds after treatment could be attributed to the reactions between the hydroxyl groups of chitosan and the aldehyde groups of the cross-linking agents. While the PCL nanofibrous scaffolds had a rather lower weight loss because of its hydrophobic property, adding olive oil to it will protect from adjacent water medium. This was responsible for lower weight loss in PCL/olive oil nanofibrous scaffolds.

Characterization of Nanofibers

The functional groups of PEO/chitosan, olive oil, PCL/olive oil and PEO/chitosan/PCL/olive oil nanofibers are characterized by Fourier Transform Infrared (FTIR) which results are shown in Figure 5. In PEO/chitosan nanofibers, a broad band at 3100-3600 cm^{-1} was assigned to N-H and O-H stretching of the polysaccharide molecules. Two bands at 1560 and 1650 cm^{-1} were attributed to the amide groups in the structure of PEO/chitosan nanofibers. The broad band appeared at 2900 cm^{-1} was due to the CH_2 stretching groups. The C-H group peaks were observed at 1340 and 1370 cm^{-1}. The absorption bands around 1100 cm^{-1} assigned to C-O-C stretching vibration. In PCL/olive oil nanofibers, the broad peak at 3440 cm^{-1} was due to the hydrogen banded O-H stretching. The peaks at 2859 and 2927 cm^{-1} were due to the C-H groups on the structure of PCL/olive oil electrospun nanofibers. The peak located at 1727 cm^{-1} was assigned to stretching vibration of -CH_2- bands. The CH= and C=C peaks of olive oil were observed at 3007 and 1654 cm^{-1}, respectively. These peaks in the structure of PCL/olive oil indicated that olive oil was embedded within the PCL/olive

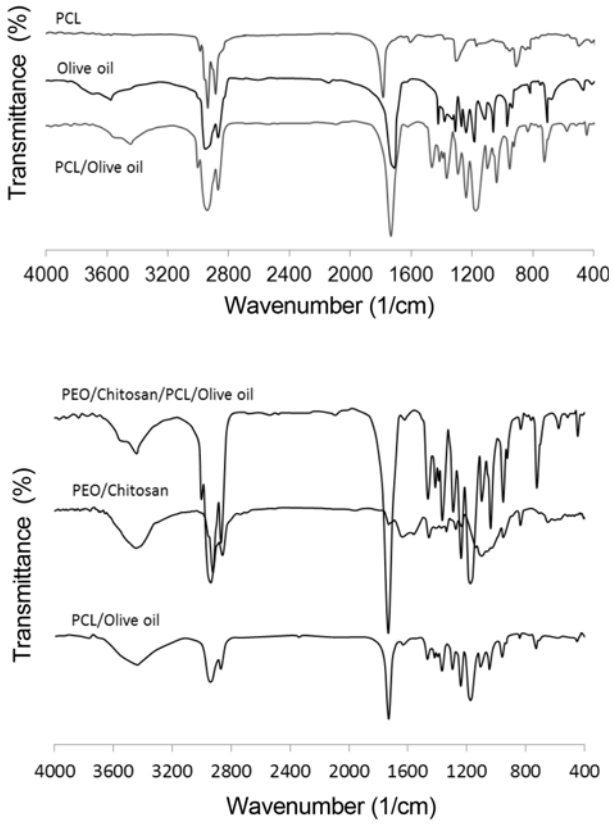

Figure 5. FTIR spectra of electrospun nanofiber scaffolds.

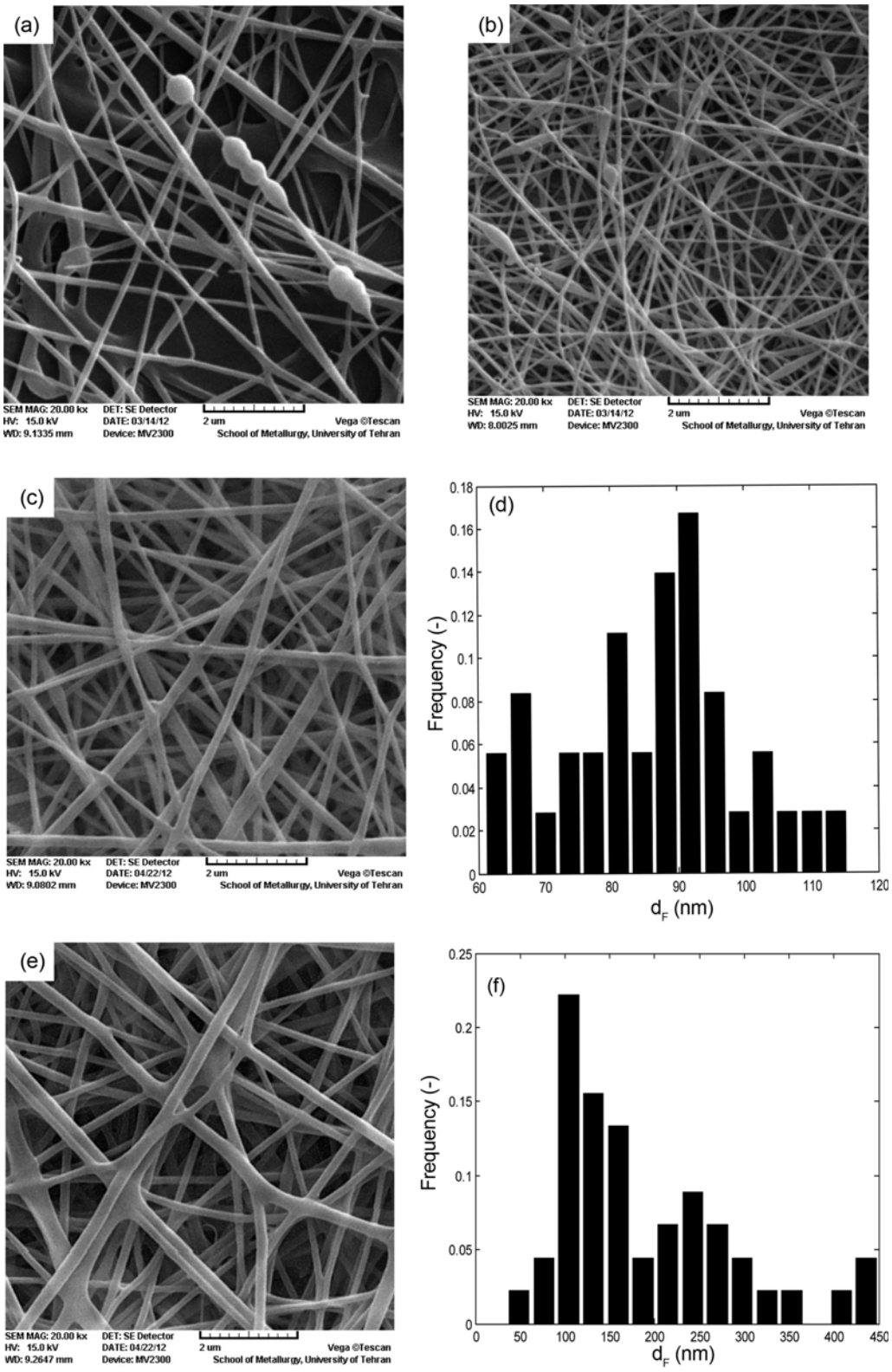

Figure 6. The SEM images of PEO/chitosan/PCL/olive oil electrospun nanofibers at different conditions of electrospinning parameters including (a) voltage 15 kV, distance 7.5 and flow rate 0.6), (b) voltage 20 kV, distance 13.75 cm and flow rate 0.6), (c) optimum conditions, (d) distribution of fiber diameters, (e) cross-linked nanofibers at optimum condition, and (f) distribution of fiber diameters of cross-linked nanofibers.

oil composite nanofibers. Other characteristic peaks of olive oil overlapped with PCL. The FTIR spectra of PEO/chitosan/PCL/olive oil showed that the amide groups of chitosan with weaken intensity were shifted to the lower wave numbers (i.e. from 1650 to 1638.9 cm^{-1}). The changes in FTIR spectra of PEO/chitosan/PCL/olive oil composite nanofibers indicated that there is no detectable chemical banding between PEO/chitosan and PCL/olive oil, except of presence of possible molecular interaction between PEO/chitosan and PCL/olive oil [37].

The SEM images of PEO/chitosan/PCL/olive oil electrospun nanofibers at different conditions of electrospinning parameters are shown in Figure 6. Comparison of mean fiber diameter in Figure 6(a) (characterized by; voltage 15 kV, distance 7.5 and flow rate 0.6) to Figure 6(b) (voltage 20 kV, distance 13.75 cm and flow rate 0.6) indicated that the interaction of voltage and distance at the time was more important than effect of other interaction terms. Also, the SEM image and distribution diameter of PEO/chitosan/PCL/olive oil composite nanofibers at optimum conditions of electrospinning parameters before and after cross-linkage by moist GTA vapor for 24 h, are shown in Figure 6(c)-(f). The results confirmed that the obtained average diameters of the non-cross linked and cross-linked fibers were 86±13 and 188±50 nm, respectively. The results indicated that the fiber diameter and fiber size distribution increased after cross-linking by GTA. A similar trend was reported for GA cross-linking studies that have been performed on chitosan nanofibers [38].

The SEM images of PCL/olive oil nanofibers with weight ratio of 1:10, 2:10 and 3:10 are shown in Figure 7. As can be seen, the homogeneous fibers were formed at optimum conditions of electrospinning process and weight ratios of 1:10 and 2:10 (average diameter were 273 and 285 nm). When the weight ratio of PCL to olive oil was increased to 3:10, the electrospun of PCL/olive oil nanofibers was difficult to be formed which resulted in formation of beads and droplets alongside the fibers.

Olive Oil Release Study from Nanofibrous Scaffolds

The release characteristic of olive oil upon cross-linked PEO/chitosan/PCL/olive oil nanofibers is investigated by the total immersion method in the releasing media during 24 h which result is presented in Figure 8. As shown, the fast release occurred during the first 3 h, and increased gradually afterwards to maximum 12 h. The significant factors contributing to drug release in controlled release systems is the behavior of the matrix loaded with the drug in the release medium. In the experiments, when scaffold sample was exposed to a liquid medium, the olive oil on the inner layers of scaffold begun to wash out and slightly dissolved. After that, the scaffolds begun to swell and weight loss occurred. As a result, the high degree of swelling along with the dissolution and washing of the nanofibrous scaffolds caused a quick burst release. Over time, the liquid phase had enough time to penetrate into the interior layers and reached a balance.

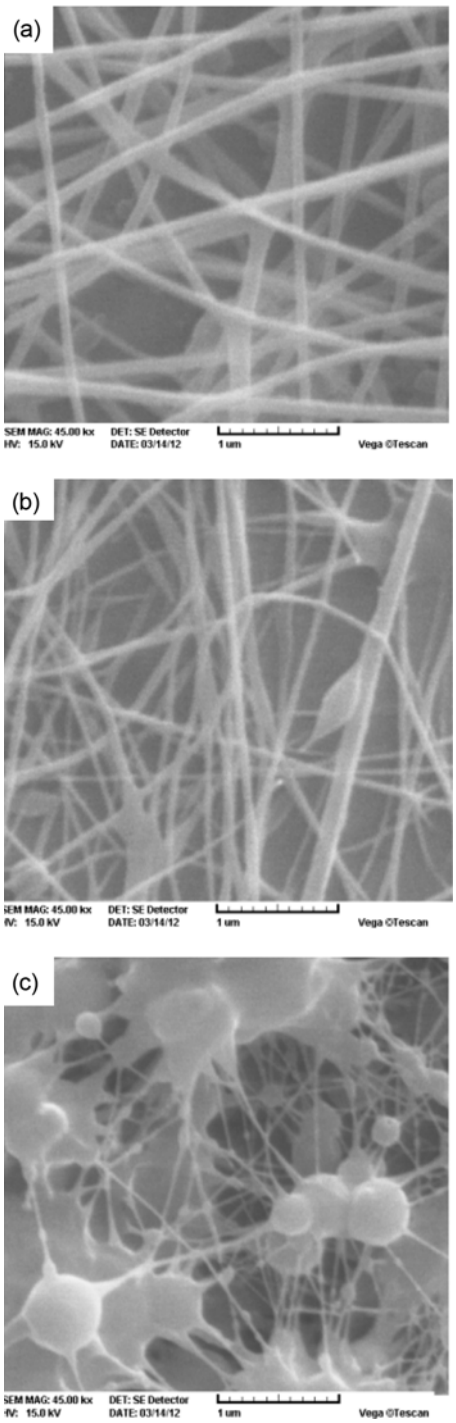

Figure 7. SEM images of PCL/olive oil nanofibers with different concentrations of olive oil; (a) 1 %, (b) 2 %, and (c) 3 %.

Cell Adhesion Studies

Cytotoxicity, Cell Adhesion, and Proliferation

Cytotoxicity of the prepared nanofibrous scaffolds was

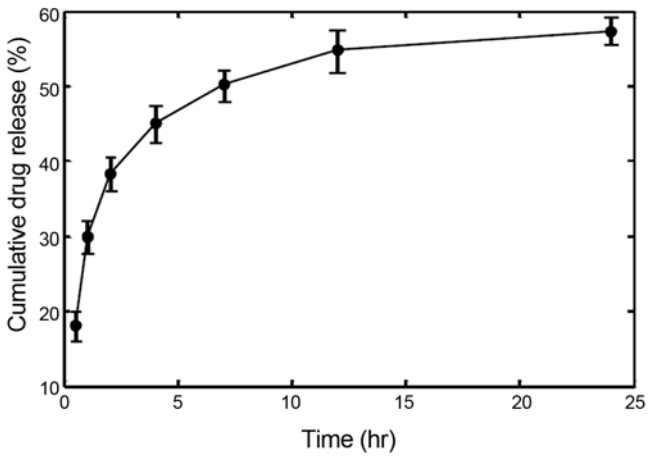

Figure 8. Cumulative release profiles of olive oil from cross-linked PEO/chitosan/ PCL/olive oil nanofibrous scaffold.

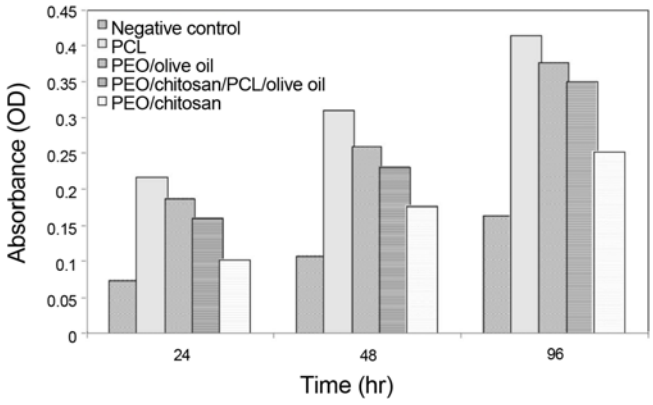

Figure 9. Cytotoxicity studies on PCL, PCL/olive oil, PEO/chitosan (cross-linked), PEO/chitosan/PCL/olive oil (cross-linked) nanofibrous scaffolds, and negative control using HDF at 24, 48, and 96 hrs of attachment.

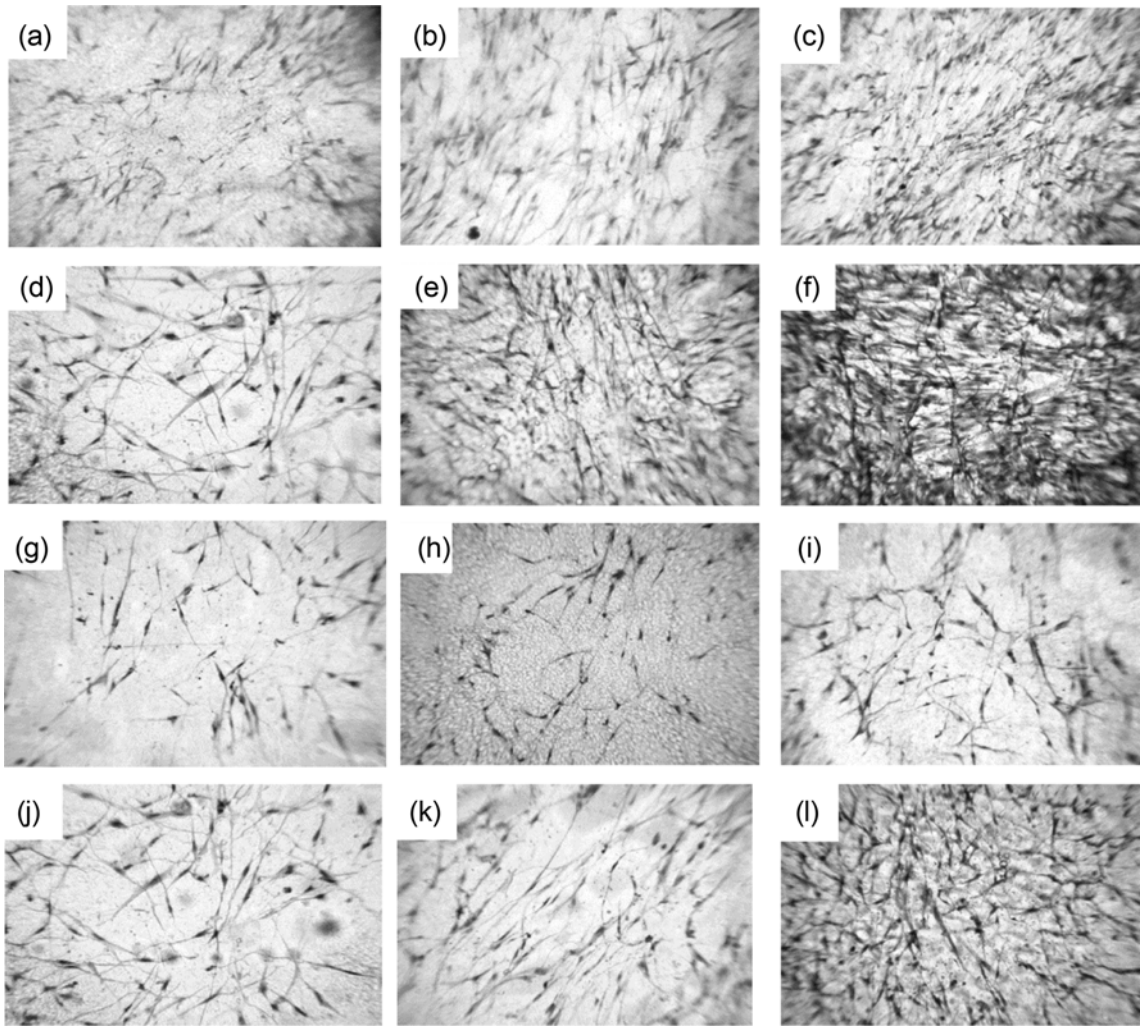

Figure 10. Cell culture studies on PCL (a) 24 hrs, (b) 48 hrs, (c) 96 hrs, PCL/Olive oil (d) 24 hrs, (e) 48 hrs, (f) 96 hrs, PEO/chitosan (cross-linked) (g) 24 hrs, (h) 48 hrs, (i) 96 hrs, and PEO/chitosan/PCL/olive oil (cross-linked) nanofibrous scaffolds (j) 24 hrs, (k) 48 hrs, and (l) 96 hrs.

analyzed using MTT assay in vitro after 24, 48 and 96 h which results are presented in Figure 9. As shown, the absorbance intensity of the tested scaffolds increased with the increase of culture time. The absorbance intensities, after 96 hrs, showed comparatively higher values with respect to negative control, which evidently showed the non toxic behavior of the nanofibrous scaffolds. Increase in the absorbance intensities, as a direct index of the living cells numbers, clearly addressed the cell proliferation. However, the PCL-containing nanofibrous scaffolds had good biological properties for cell attachment, growth and proliferation in comparison to others nanofibrous scaffolds.

Cell Attachment Morphology

The Attachment morphology study was conducted with HDF cells by Hematoxylin and eosin (H&E) staining for three time intervals (Figure 10). The HDF cells showed spread morphology at higher incubation periods (96 hr) for tested nanofibrous scaffolds. However, HDF cells showed good attachment and spreading on the nanofibrous scaffold of the PCL-containing nanofibrous scaffolds in comparison to others prepared scaffolds. As expected, the area covered with HDF cells of different scaffolds increased with the increase of culture time. Since the cells behavior indicated good attachment and spreading on the nanofibrous scaffold of PEO/chitosan/PCL/olive oil, it is promised that prepared nanofibrous scaffold could be used as an alternative vehicle for wound dressing applications.

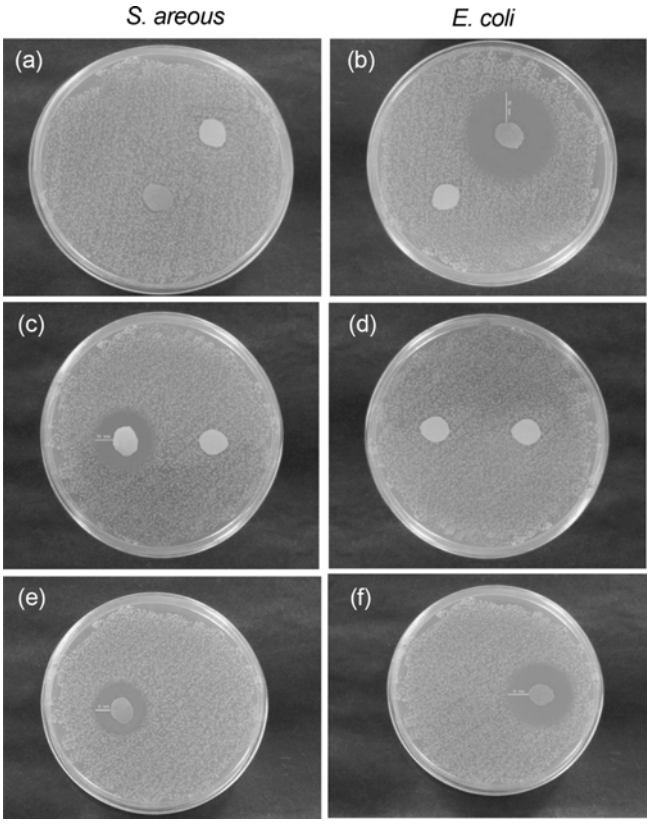

Figure 11. Antibacterial activity against *E. coli* and *S. areous* bacteria for (a) and (b) PEO and PEO/chitosan, (c) and (d) PCL and PCL/olive oil, and (e) and (f) PEO/chitosan/PCL/olive oil composite nenofibrous scaffolds.

Antibacterial Activity

The antibacterial activity of prepared nanofibers are shown in Figure 11. As shown in Figures 11(a) and (b), the pure PEO nanofibers did not shown any antibacterial activity against *E. coli* and *S. aureus*. By contrast, the PEO/chitosan nanofibers had excellent bacterial efficiency to Gram-negative bacteria *E. coli*, meanwhile, they did not show any suitable response against Gram-positive bacteria *S. aureus*. Figures 11(c) and (d) demonstrated that the PCL nanofibers lacking olive oil had no significant antibacterial activity. Conversely, the PCL/olive oil nanofibrous scaffolds had higher bacterial activity against *S. aureus*, while the PCL/olive oil nanofibrous scaffolds did not show any sign of antibacterial activity against *E. coli*. On the other hands, PEO/chitosan/PCL/olive oil composite nanofibrous scaffolds had antibacterial properties to the both Gram-negative and Gram positive microorganisms (Figures 11(e) and (f)).

Conclusion

In the present study, composite nanofibers of PEO/chitosan/PCL/olive oil were successfully fabricated via electrospinning process. The structure and morphology of electrospun nanofibers were determined using Fourier Transform Infrared (FTIR) and Scanning Electron Microscopy (SEM), respectively. The response surface methodology based on Box-Behnken design was used to determine the relation of process parameters on the diameter of electrospun nanofibers. Three factors of electrospinning process including, voltage, TCD and flow rate at three levels for fabrication of 21.2 kV, flow rate of 0.2 m*l* hr^{-1} and TCD of 14.3 cm, the predicted minimum value of fiber diameter was found to be 88 nm. This data was in a good match with experimental data of 86 nm. The incorporation of different weight percentages of olive oil onto the electospun nanofibers indicated that the optimum weight percentage of olive oil was 2 %. In vitro release behavior of olive oil from PEO/chitosan/PCL/olive oil composite nanofibrous scaffolds suggested that olive oil was released from composite nanofibers with about 58.1 % of total olive oil encapsulation released after one day study. The cells attachment studies showed comparatively good attachment and spreading on the prepared nanofibrous scaffolds. Cytotoxicity results addressed the cell proliferation and non toxic behavior of the nanofibrous scaffolds. The high antibacterial activity of PEO/chitosan/PCL/olive oil composite nanofibers suggest an optimized nanofibrous scaffold may be useful for wound dressing.

References

1. I. S. Chronakis, *J. Mater. Proc. Technol.*, **167**, 283 (2005).
2. A. J. Meinel, O. Germershaus, T. Luhmann, H. P. Merkle, and L. Meinel, *Eur. J. Pharm. Biopharm*., **81**, 1 (2012).
3. P. Nakielski, T. Kowalczyk, K. Zembrzycki, and T. A. Kowalewski, *J. Biomed. Res. Part B*, **103**, 282 (2015).
4. J. S. Im, J. Yun, Y. M. Lim, H. I. Kim, and Y. S. Lee, *Acta Biomater.,* **6**, 102 (2010).
5. B. Song, C. Wu, and J. Chang, *J. Biomed. Res. Part B*, **100**, 2178 (2012).
6. Y. N. Lin, K. M. Chang, S. Jeng, P. Y. Lin, and R. Q. Hsu, *J. Mater. Sci.-Mater. Med.*, **22**, 571 (2010).
7. J. Venugopal, S. Low, A. T. Choon, and S. Ramakrishna, *J. Biomed. Res. Part B*, **84**, 34 (2010).
8. P. C. Caracciolo, V. Thomas, Y. K. Vohra, F. Buffa, and G. A. Abraham, *J. Mater. Sci.-Mater. Med.*, **20**, 2129 (2009).
9. C. Xu, C. Lei, L. Meng, C. Wang, and Y. Song, *J. Biomed. Res. Part B*, **100**, 1435 (2012).
10. H. Zhou, A. H. Touny, and S. B. Bhaduri, *J. Mater. Sci.-Mater. Med.*, **22**, 1183 (2011).
11. V. Leung, R. Hartwell, S. S. Elizei, H. Yang, A. Ghahary, and F. Ko, *J. Biomed. Res. Part B*, **102**, 508 (2014).
12. K. T. Shalumon, K. H. Anulekha, V. Sreeja, S. V. Nair, K. P. Nair, and R. J. Chennazhi, *Int. J. Biol. Macromol.*, **49**, 247 (2011).
13. D. S. Katti, K. W. Robinson, F. K. Ko, and C. T. Laurencin, *J. Biomed. Res. Part B*, **70**, 286 (2004).
14. S. Y. Gu, Z. M. Wang, J. Ren, and C. Y. Zhang, *Mater. Sci. Eng. C*, **29**, 1822 (2009).
15. T. J. Sill and H. A. Recum, *Biomaterials*, **29**, 1989 (2008).
16. Y. Zhang, C. T. Lim, S. Ramakrishna, and Z. Huang, *J. Mater. Sci.-Mater. Med.*, **16**, 933 (2005).
17. R. Salehi, M. Irani, M. Eskandani, K. Nowruzi, S. Davaran, I. Haririan, *Int. J. Polym. Mater. Polym. Biomat.*, **63**, 609 (2014).
18. K. T. Shalumon, N. S. Binulal, N. Selvamurugan, S. V. Nair, M. Deepthy, T. Furuike, H. Tamura, and R. Jayakumar, *Carbohydr. Polym*. **77**, 863 (2009).
19. U. S. Sajeev, A. K. Anoop, M. Deepthy, and S. V. Nair, *Bull. Mater. Sci.*, **31**, 343 (2008).
20. N. S. Binulal, M. Deepthy, N. Selvamurugan, K. T. Shalumon, S. Suja, M. Ullas, R. Jayakumar, and S. V. Nair, *Tissue Eng. Part A*, **16**, 393 (2010).
21. Y. T. Jia, J. Gong, X. H. Gu, H. Y. Kim, J. Dong, and X. Y. Shen, *Carbohydr. Polym*., **67**, 403 (2007).
22. K. T. Shalumon, K. H. Anulekha, C. M. Girish, S. V. Prasanth, and R. J. Nair, *Carbohydr. Polym*., **80**, 413 (2010).
23. Y. S. Zhou, D. Z. Yang, and J. Nie, *Chinese Chem. Lett*., **18**, 118 (2007).
24. P. Zahedi, I. Rezaeian, S. O. RanaeiSiadat, S. H. Jafari, and P. Supaphol, *Polym. Adv. Technol.*, **21**, 77 (2010).
25. C. K. S. Pillai and C. P. Sharma, *Biomater. Artif. Organs,* **22**, 179 (2009).
26. X. Y. Li, X. Y. Kong, S. Shi, X. H. Wang, G. Guo, F. Luo, X. Zhao, Y. Q. Wei, and Z. Y. Qian, *Carbohydr. Polym*., **82**, 904 (2010).
27. J. Han, T.-X. Chen, C. J. B. White, and L. M. Zhu, *Int. J. Pharm.*, **382**, 215 (2009).
28. T. Wang, X. K. Zh, X. T. Xue, and D. Y. Wu, *Carbohydr. Polym*., **88**, 75 (2012).
29. R. Gurfinkel, M. Palivatkel-Naima, R. Gleisinger, L. Rosenb, and J. Singer, *Am. J. Emerg. Med*., **30**, 79 (2012).
30. Z. X. Cai, X. M. Mo, K. H. Zhang, L. P. Fan, A. L. Yin, C. L. He, and H. S. Wang, *Int. J. Mol. Sci.*, **11**, 3529 (2010).
31. S. Pandamooz, A. Hadipour, H. Akhavan-Niaki, M. Pourghasem, Z. Abedian, A. M. Ardekani, M. Golpour, M. H. Zuhair, and A. Mostafazadeh, *Biotechnol. Appl. Biochem.,* **59**, 254 (2012).
32. T. Mosmann, *J. Immunol. Methods*, **65**, 55 (1983).
33. C. Srisitthiratkul, V. Pongsorrarith, and N. Intasanta, *Appl. Surf. Sci.*, **257**, 8850 (2011).
34. L. D. Tijing, M. T. G. Ruelo, A. Amarjargal, H. R. Pant, C.-H. Park, and C. S. Kim, *Mater. Chem. Phys.*, **134**, 557 (2012).
35. Y. Park, I. H. Lee, and G. N. Bea, *J. Ind. Eng. Chem.,* **14**, 707 (2008).
36. S. H. Tan, R. Inai, M. Kotaki, and S. Ramakrishna, *Polymer*, **46**, 6128 (2005).
37. N. Sultana, M. I. Hassan, and M. M. Lim, "Composite Synthetic Scaffolds for Tissue Engineering and Regenerative Medicine", pp.13-24, Springer International Publishing, Berlin, 2015.
38. S. Sarmila, S. Abhishek, N. Rajashree, A. R. Phani, and P. L. Nayak, *Carbohydr. Polym*., **80**, 413 (2009).